

Review

# Prospects of Using Fe-Ga Alloys for Magnetostrictive Applications at High Frequencies

Vasily Milyutin <sup>1,2,\*</sup> , Radovan Bureš <sup>1</sup>  and Maria Fáberová <sup>1</sup>

<sup>1</sup> Institute of Materials Research, Slovak Academy of Sciences, Watsonova 47, 040 01 Kosice, Slovakia; rbures@saske.sk (R.B.); mfaberova@saske.sk (M.F.)

<sup>2</sup> Institute of Metal Physics, Ural Branch of Russian Academy of Sciences, Sofia Kovalevskaya 18, 620108 Ekaterinburg, Russia

\* Correspondence: v.a.milyutin@gmail.com

**Abstract:** Fe-Ga is a promising magnetostrictive rare-earth free alloy with an attractive combination of useful properties. In this review, we consider this material through the lens of its potential use in magnetostrictive applications at elevated frequencies. The properties of the Fe-Ga alloy are compared with other popular magnetostrictive alloys. The two different approaches to reducing eddy current losses for such applications in the context of the Fe-Ga alloy, in particular, the fabrication of thin sheets and Fe-Ga/epoxy composites, are discussed. For the first time, the results of more than a decade of research aimed at developing each of these approaches are analyzed and summarized. The features of each approach, as well as the advantages and disadvantages, are outlined. In general, it has been shown that the Fe-Ga alloy is the most promising magnetostrictive material for use at elevated frequencies (up to 100 kHz) compared to analogs. However, for a wide practical application of the alloy, it is still necessary to solve several problems, which are described in this review.

**Keywords:** Fe-Ga alloy; magnetostriction; magnetostrictive materials; elevated frequencies; AC magnetic properties; rolling; magnetostrictive composites



**Citation:** Milyutin, V.; Bureš, R.; Fáberová, M. Prospects of Using Fe-Ga Alloys for Magnetostrictive Applications at High Frequencies. *Condens. Matter* **2023**, *8*, 80. <https://doi.org/10.3390/condmat8030080>

Academic Editor: Ali Gencer

Received: 31 July 2023

Revised: 4 September 2023

Accepted: 5 September 2023

Published: 8 September 2023



**Copyright:** © 2023 by the authors. Licensee MDPI, Basel, Switzerland. This article is an open access article distributed under the terms and conditions of the Creative Commons Attribution (CC BY) license (<https://creativecommons.org/licenses/by/4.0/>).

## 1. Introduction

Magnetostrictive materials play an important role in modern electrical engineering. Typical devices based on such materials are various sensors [1], actuators [2], transducers [2,3], and vibration energy harvesters [4]. Additionally, they can be used in various biomedical applications [5] and in flexible electronics [6,7]. A significant part of these applications involves operation in conditions of elevated remagnetization frequencies (from one up to hundreds of kHz). Such application conditions have their specifics and dictate additional requirements for materials. This is mainly due to the need to deal with eddy current losses, which become a serious problem with increasing remagnetization frequency. To minimize eddy current losses, various engineering approaches are used to reduce the continuous volume of a conductive ferromagnetic material, for example, slicing. These approaches have their specifics and limitations depending on the magnetostrictive material used, which must be investigated for each case. This information is necessary to develop optimal modes for manufacturing magnetostrictive devices with the best performance and energy efficiency. Additionally, of course, the properties of the magnetostrictive material itself are also important, which determine the behavior at elevated frequencies. Thus, to create magnetostrictive devices based on a certain alloy, complex studies are required both on the specifics of using various engineering approaches to reduce eddy current losses and on the AC magnetic properties of the material.

Traditionally, the most common magnetostrictive alloys used on an industrial scale are FeTbDy (Terfenol-D) and FeCo. In recent years, the Fe-Ga alloy has also gained popularity. It combines higher magnetostriction than FeCo and much lower saturation fields and cost compared to FeTbDy. In addition, it has many other advantages, such as good temperature

stability, corrosion resistance, the possibility of tailoring properties in wide intervals due to structure control, and others [8–10]. Since the discovery of high magnetostriction in the Fe-Ga alloy by Clark et al. [11], this alloy consistently attracts increased attention from researchers and engineers, which is confirmed by publication dynamics (Figure 1).

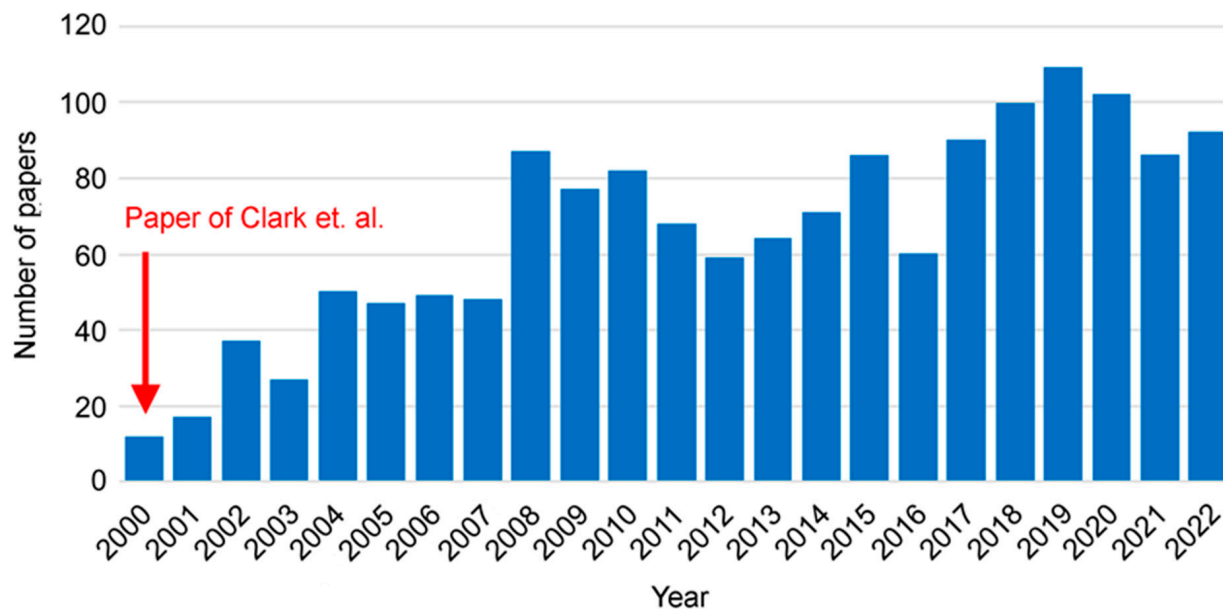


**Figure 1.** Papers devoted to Fe-Ga alloy in the Web of Science core collection scaled by 0.8 to correct for an average rate of errors [11].

In the initial stages of research, they were mainly aimed at studying the structural features of the alloy to reveal the mechanisms of the anomalous increase in iron magnetostriction upon the addition of gallium. To date, a sufficient amount of information has been obtained regarding the optimal methods for manufacturing an alloy and methods for increasing magnetostriction. As the next stage in the development of the material and the next step toward its industrial application, research is needed in the context of the specifics of its practical use under certain conditions. This review considers the prospects and features of using the Fe-Ga alloy for AC applications at elevated frequencies.

Based on this alloy, some experimental magnetostrictive devices operating at elevated frequencies, such as sound and ultrasound transducers [12,13], underwater transducers [14], magnetostrictive vibrators [12,15], and others, are already being prepared and tested. It should also be noted that magnetostrictive energy harvesters [4] are considered a promising direction for the practical use of the Fe-Ga alloy. In recent years, a large number of papers, both experimental and theoretical, have been published in this direction [16–19]. It was shown that, due to the optimal combination of its magnetic and mechanical properties, the Fe-Ga alloy can be successfully used in energy harvesters of various types, which are capable of efficiently converting mechanical vibration energy into an electrical one. However, to expand the range of possible applications and achieve the best performance of devices, as well as scaling to the industry, complex research is needed to study the features of the manufacture and use of Fe-Ga at elevated frequencies. To date, there are scattered studies on this issue. In this review, for the first time, the previously obtained information is summarized and analyzed; in addition, directions for further research are proposed.

## 2. Comparison of AC Functional Properties of Fe-Ga with the Most Common Magnetostrictive Alloys

First, it is necessary to analyze the properties of the Fe-Ga alloy, which are important from the point of view of applications at elevated frequencies, and compare them with the most common analogs. It should be noted that in this article, we are talking about an alloy

with a gallium content of about 19 at. %, i.e., near the first peak of magnetostriction on the plot of magnetostriction versus composition [20]. In terms of the ratio between the price of the chemical elements of the alloy and the magnitude of the magnetostriction, Fe-Ga and FeGaRE (RE = rare earth element) alloys are the optimal solution compared to the many binary and ternary magnetostrictive alloys (Figure 2). Of course, it is not the only important criterion. The Fe-Ga alloy, although significantly inferior to TbDyFe in terms of magnetostriction, has many other advantages, which are discussed below. A comparison of the main properties of common magnetostrictive alloys Fe<sub>2</sub>Tb<sub>0.3</sub>Dy<sub>0.7</sub> (Terfenol-D), Fe<sub>30</sub>Co<sub>70</sub>, and Fe<sub>81</sub>Ga<sub>19</sub> is shown in Table 1. In addition, a representative of a promising group of magnetostrictive materials, FeGaRE, has been added to the comparison, namely (Fe<sub>81</sub>Ga<sub>19</sub>)<sub>99.8</sub>Tb<sub>0.2</sub>. It is well known that small additions of rare earth elements have a positive effect on the magnetostriction of the alloy without significant price increases [21,22]; therefore, such alloys are considered promising replacements for binary Fe-Ga. The identification of the physical reasons for the increase in Fe-Ga magnetostriction upon the addition of rare earth elements is still the subject of many studies [8,23–25].

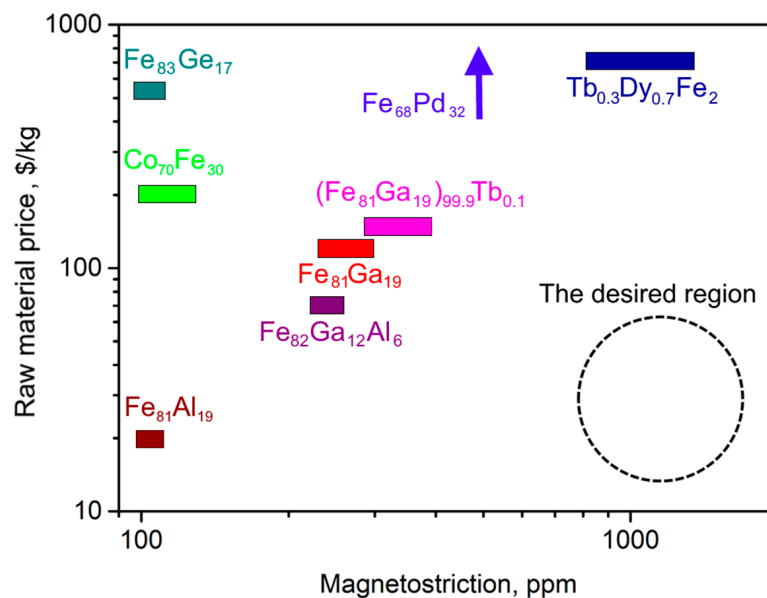


**Figure 2.** The comparison of classical binary and ternary magnetostrictive alloys in terms of the ratio between the price of alloy chemical elements and magnetostriction in single-crystal or highly textured polycrystal. Magnetostriction values are taken from the literature [26–33]. The scattering of magnetostriction values is related to the dependence on the method of obtaining samples and heat treatment, as well as measurement conditions. Actual prices of metals were taken from open web resources.

**Table 1.** Comparison of several common magnetostrictive alloys in terms of the main properties important in the context of their use at elevated frequencies. Data taken from literary sources [34–38]. The information for bulk as cast polycrystalline samples is preferably used. Rounded data are given.

Alloy	Coercivity, A/m	Saturaion Field, kA/m	Electrical Resistivity, μΩ·cm	Real Part of Complex Permeability at 10 kHz
Fe <sub>81</sub> Ga <sub>19</sub>	≈100	≈18	100	50
(Fe <sub>81</sub> Ga <sub>19</sub> ) <sub>99.8</sub> Tb <sub>0.2</sub>	≈200	≈40	135	35
Fe <sub>30</sub> Co <sub>70</sub>	≈1000	≈40	33 *	16
Terfenol-D	≈2000	≈160	60	10

\* Calculated value using JMatPro.

First of all, the magnitude of the coercivity and the magnetic field, which is necessary to apply to achieve the maximum magnetostriction, are compared. These properties are extremely important in the context of the practical application of magnetostrictive alloys. A low coercivity is necessary to minimize the hysteresis component of magnetic losses. At the same time, the weaker the magnetic field is required to saturate the material, the easier it is to create miniature and energy-efficient devices on its basis. In terms of coercivity, Fe-Ga is noticeably superior to analogs and has an order of magnitude lower values (Table 1). It should be noted that this parameter is very sensitive to the structural state, the number of defects, and the purity of the chemical elements used. The value can vary greatly in different experiments depending on the conditions of sample preparation, so the table shows approximate averaged data. However, the trend of much lower coercivity in Fe-Ga alloys persists in all cases. The same is true for the saturation field, which also depends on which sample was measured (single crystal or polycrystal), its orientation (in the case of a single crystal) or crystallographic texture (in the case of a polycrystal), the level of micro-distortions, and chemical purity. Moreover, due to the demagnetizing factor, the shape and size of the samples play an important role and significantly affect the magnetostriction curves as a function of the magnetic field. In this case, again, Fe-Ga shows the best result, although the difference with FeCo is not so significant. Addition of 0.2 at. % Tb also leads to a significant increase in the saturation field.

In addition to magnetostriction and AC magnetic properties, an important parameter is electrical resistivity  $\rho$ . It is not a functional property of magnetostrictive alloys and is not important in the case of near-DC applications; however, with an increase in operating frequencies, its importance increases dramatically. This is because this property largely determines the eddy current losses, which are inversely proportional to the electrical resistivity value. In addition,  $\rho$  affects the processes of dynamic magnetization reversal and the resonant frequency since, in a conductive ferromagnetic material, the moving domain walls are mainly retarded by eddy current damping [39]. The binary Fe<sub>81</sub>Ga<sub>19</sub> alloy has a relatively high electrical resistivity for a metal compound (Table 1). The reason is that the alloy mainly has the structure of a solid solution in which gallium atoms replace iron atoms in the  $\alpha$ -Fe lattice. Given the significant difference in the size of the atoms, this leads to the appearance of lattice distortions, which reduces the electron mean free path and increases the electrical resistivity [40]. Moreover, a further increase in the  $\rho$  value is possible due to the alloying of the binary alloy with various elements such as Mn [41] or RE [36]. For example, the addition of 0.2% Tb leads to an increase of more than 30% compared to a binary alloy (Table 1). Other magnetostrictive alloys used for comparison have much lower electrical resistivity, which is associated with an ordered structure in the case of Fe<sub>2</sub>Tb<sub>0.3</sub>Dy<sub>0.7</sub> and the lack of difference in the size of atoms of Fe (124 pm) and Co (125 pm) [42] in case of a Fe<sub>30</sub>Co<sub>70</sub> solid solution.

Finally, we compared the magnetic permeability of alloys at elevated frequencies. For this, we used the real part of complex relative permeability  $\mu_r'$  at room temperature. This is an important parameter that reflects how easy it is to magnetize a material at a certain frequency. As the remagnetization frequency increases, the value of  $\mu_r'$  decreases, so it is important to control it in the region of frequencies of interest. Table 1 shows values at 10 kHz. It can be seen that the Fe-Ga alloy again outperforms the others. The addition of Tb reduces the permeability of a binary alloy but increases the resonant frequency [43].

### 3. Engineering Solutions for High-Frequency Applications of Fe-Ga

As noted earlier, traditionally, the creation of high-frequency magnetic (including magnetostrictive) devices is based on a simple idea, which consists of reducing the continuous cross-section area of the conductive material that is perpendicular to the applied field. It should be noted that, depending on the purpose, the Fe-Ga alloy is obtained in the form of a wide range of different products, some of which, among other things, can be used at elevated frequencies, e.g., amorphous ribbons [21], thin films [44], wires [45], and rods [46]. For example, thin films are in a promising direction and appropriate for high-frequency ap-

plications due to their very low thickness of  $<1 \mu\text{m}$  and deserve a separate study. However, this review focuses on the possibilities of creating bulk magnetostrictive devices based on the Fe-Ga alloy, which can perform certain (including mechanical) work at elevated frequencies. One more important criterion is the low cost of manufacturing technology and the possibility of scaling into the industry. Therefore, we do not consider the slicing (cutting into thin slices) of single crystals approach since the use of single crystals entails a significant increase in costs. In some individual cases, this may be justified, but much cheaper polycrystals are needed for widespread industrial use. In addition, the absence of grain boundaries in a single crystal is a negative factor from the point of view of applications at higher frequencies [47]. Slicing of polycrystals is a weakly efficient approach because it does not allow the creation of necessary crystallographic texture, the importance of which is described in more detail below. There are two main directions for the manufacture of bulk magnetostrictive products suitable for applications at elevated frequencies. They are laminated stacks and metal/insulator composites (Figure 3), both of which are appropriate for Fe-Ga. Each of these approaches has its specifics, advantages, and disadvantages. In this article, we consider both of them.

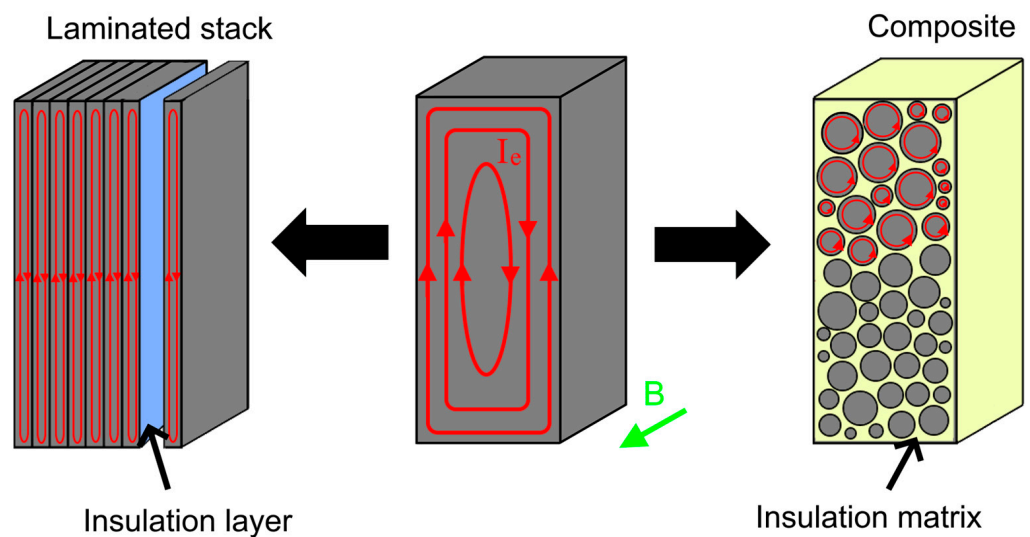


**Figure 3.** Schematic representation of approaches used to reduce eddy current losses. The red arrows schematically show the eddy currents that occur in the material when an AC magnetic field is applied.

### 3.1. Laminated Stacks

The manufacturing technology of magnetostrictive laminated stacks was borrowed from Fe-3% Si electrical steel, which has been widely used in this form for many years. It can also be used in the case of the Fe-Ga alloy [48]. For the manufacture of laminated stacks, relatively thin sheets of Fe-Ga (0.5 mm and thinner) are used, which are coated with an electrical insulator (for example, MgO) and put together into a three-dimensional product. The optimal way to obtain thin sheets, both in terms of the availability of technology and the possibilities that they provide, is rolling and subsequent heat treatment. The main advantage of rolling over the simple cutting of an ingot into slices is the ability to change the grain structure and, more importantly, the crystallographic texture. The presence of a certain crystallographic texture in the Fe-Ga alloy is a critical condition for achieving high values of magnetostriction due to pronounced anisotropy [49]. At the micro level, the  $\text{Fe}_{81}\text{Ga}_{19}$  alloy usually has a body-centered cubic structure. A noticeable amount of other phases is possible only with extremely long annealing of several hundred hours [50], so they can be neglected. There are three main crystallographic directions in the cubic structure:  $\langle 100 \rangle$ ,  $\langle 110 \rangle$ , and  $\langle 111 \rangle$ . It is known that in the  $\text{Fe}_{81}\text{Ga}_{19}$  alloy, the magnetostriction constant  $\lambda_{100}$  is maximum and is about 250 ppm. At the same time,  $\lambda_{110}$  is also quite high (about 150 ppm). And finally,  $\lambda_{111}$  is minimal and, according to various sources, varies from

–20 to 0 [51–53]. Thus, the optimal texture is one that contains as many  $\langle 100 \rangle$  directions as possible along some external direction (for example, the rolling direction) and, at the same time, the minimum content of  $\langle 111 \rangle$  directions. It has been experimentally established that the value of magnetostriction in a sheet correlates well with the content of these texture components [52,54,55]. It should be noted that the creation of a texture of this type in a bcc alloy is a rather difficult task. In recent years, attempts have been made to actively solve this problem by studying the mechanisms of texture formation in Fe-Ga [53,56] and the selection of deformation and recrystallization parameters [52,53,55,57–65]. In terms of technology, there are two approaches to creating desirable texture in Fe-Ga sheets. The most popular direction is the creation of the so-called Goss texture  $\{110\}\langle 100 \rangle$  and close to it using the technology of secondary recrystallization [52,64,66–73]. This technology has previously proven itself well in the production of grain-oriented FeSi sheets and has also shown its effectiveness in the case of Fe-Ga. Its essence lies in the introduction of special nanosized inhibitors into the composition of a binary alloy, which are usually carbides [52], borides [61], or sulfides [74]. Distributed along grain boundaries, they inhibit grain growth during primary recrystallization, thereby inhibiting the development of unfavorable texture components, which grow most intensively under normal conditions. Due to this, favorable conditions are formed for the abnormal growth of the  $\langle 100 \rangle\{110\}$  component during subsequent high-temperature annealing (1000–1300 °C), which makes it possible to overcome pinning centers. In addition, in order to additionally stimulate the development of such a texture due to the difference in surface energy [75] (so-called surface-energy-induced selective grain growth), secondary recrystallization is carried out in a special atmosphere enriched with hydrogen [64] or sulfur [52,67]. More detailed information regarding the technology and mechanisms of texture formation can be found elsewhere [76]. The purpose of these studies in relation to the Fe-Ga alloy is to approach the one-component Goss texture in sheets, and, as a result, the magnetostriction value close in magnitude to a single crystal. For this, deformation modes, temperature, time, heating rate, and atmosphere during annealing are usually varied. In the last few years, approaches have been developed that allow achieving an ideal Goss texture in Fe-Ga sheets, for example, due to twin roll casting, warm rolling, and high-temperature annealing, magnetostriction of the order of 200 ppm was achieved in sheets with a thickness of 0.5 mm [72]. Unfortunately, the technology for creating texture due to secondary recrystallization has several disadvantages. First, technological difficulties caused by the need to add inhibitors to the binary alloy, as well as long-term high-temperature annealing in a certain atmosphere. However, a more serious problem is the grain structure of the sheets. Abnormal grain growth during secondary recrystallization leads to the fact that the final structure contains grains reaching a size of several centimeters or more (depending on the size of the sample). This leads to the degradation of mechanical properties that are important for many applications of magnetostrictive devices that require operation under stress conditions for example the non-destructive testing based on ultrasonic guided waves [77]. In addition, large grains are unfavorable in terms of eddy current losses.

For this reason, an alternative direction is being developed, namely, the creation of the necessary crystalline texture due to primary recrystallization, which does not lead to the formation of large grains [53,54,58,59,62,63,65,78]. The main problem with this approach is the much weaker  $\langle 100 \rangle // \text{RD}$  (rolling direction) texture compared to secondary recrystallization. However, by optimizing the parameters of thermomechanical processing, it is possible to obtain a significant proportion of such a texture and an acceptable level of magnetostriction. For instance, it was shown that especially promising in this direction is cold rolling with medium deformation degrees (60–70%), which, in combination with primary recrystallization, makes it possible to achieve magnetostriction of the order of 150 ppm and good mechanical properties in sheets with a thickness of 0.5 mm [53]. In addition, an important parameter is the initial structure of the sample that is subjected to rolling. For example, the authors of [58] propose to use secondarily recrystallized sheets with Goss texture as a workpiece for further rolling (also with a medium deformation degree) and

primary recrystallization. This leads to a large proportion of the  $\{100\}\langle 001 \rangle$  cubic texture (more than 90%), an optimal grain size, and a good combination of magnetostriction and mechanical properties in ultrathin sheets  $(\text{Fe}_{83}\text{Ga}_{17})_{99.9}(\text{NbC})_{0.1}$  with a thickness of about 0.1 mm. It is also shown that, in addition to varying the parameters of deformation and annealing, the proportion of favorable texture components can be increased due to additional external influences, such as the annealing atmosphere and magnetic field [55,78]. In general, although primary recrystallization does not lead to such a sharp texture as the technology using secondary recrystallization, it has potential because, under certain conditions, it leads to an optimal combination of magnetostriction and mechanical properties. In addition, this technology is usually much simpler and cheaper.

It should be noted that there is no need to achieve 100% content of the  $\langle 100 \rangle // \text{RD}$  component in sheets during their manufacture. From the point of view of the formation of high values of magnetostriction in the sheet, it is sufficient to obtain the predominant number of such grains and minimize the content of grains with directions  $\langle 111 \rangle // \text{RD}$ . The desire to create a texture close to a single-component one usually does not pay off the efforts made since it does not provide a very large gain in magnetostriction. So, for example, samples after primary recrystallization with the content of  $\eta$  ( $\langle 100 \rangle // \text{RD}$ ) components of the order of 70% demonstrate magnetostriction 150 ppm [53], while 100% of such a texture in samples after secondary recrystallization leads to magnetostriction of the order 200 ppm [72]. In fairness, it should be noted that the magnetostriction values given in different papers cannot always be compared with each other. This is primarily due to differences in measurement methods and protocols. In addition, the composition of the samples varies slightly in different experiments (gallium content from 17 to 20% at.) as well as the alloying elements. And finally, the magnetostriction of Fe-Ga polycrystals is determined not only by the texture but also by the features of atomic ordering at the nano level [79], which is highly dependent on heat treatment [80] and may vary from experiment to experiment.

In order to obtain volumetric magnetostrictive devices, Fe-Ga sheets with optimal structure and properties should be used to create laminated stacks. To do this, it is necessary to solve a number of technical problems aimed at developing optimal modes for manufacturing such objects. In addition, it is necessary to investigate their functional properties. However, to date, such works are practically absent, except [48].

### 3.2. Metal/Insulator Composites

Magnetostrictive composites are bulk compacted objects in which ferromagnet particles are separated from each other by some kind of compound with high electrical resistivity (insulator) [81]. This approach allows for maintaining a relatively high magnetostriction but, at the same time, minimizes the intra-particles eddy current, which unlocks the possibility of use at high frequencies. It is necessary to distinguish this class of materials from magnetic elastomers, which also consist of ferromagnetic particles and an organic matrix and are also capable of changing linear dimensions when a magnetic field is applied, but due to other mechanisms [82]. In the manufacture of Fe-Ga-based magnetostrictive composites, epoxy resins are most often used as insulators [83–87] because they have suitable mechanical properties for this purpose and are also easy to use. In addition, their important advantage is that their use provides wide opportunities for particle orientation with the help of an external magnetic field during solidification, which makes it possible to increase the magnetostriction of composites. However, depending on the purpose and intended conditions of use, other options are possible, for example, polyurethane [88] or silicone [89]. A typical process for the manufacture of magnetostrictive composites consists of mixing the powder with epoxy in specified proportions, degassing, and solidifying under certain conditions (temperature and magnetic field). Sometimes, a certain pressure is applied before curing to reduce the porosity of the composites. In turn, Fe-Ga powder can be obtained in several different ways. They include milling of ingots [90], gas atomization [84], spark erosion [91], and mechanical alloying [92].

In terms of materials engineering, magnetostrictive composites are quite complex objects because there are a large number of parameters that affect properties. These parameters are the chemical and phase composition of the Fe-Ga alloy, the size, morphology, and structural state of the powder, the type and amount of insulator, the method and parameters of manufacturing the composite, as well as additional parameters such as pressure and magnetic field applied during their manufacture. For this reason, the development of magnetostrictive composites with optimal characteristics is a labor- and time-consuming process. However, an analysis of the results obtained so far allows us to identify several promising areas for the development of such materials. In recent years, it has been shown that the replacement of the binary Fe-Ga by the ternary FeGaRE alloy with a low RE content (up to 3 at. %) in magnetostrictive composites allows for the achievement of a significant increase in magnetostriction [93,94]. Moreover, based on the data [36], it can be assumed that this can also improve frequency stability and reduce core loss at higher reversal frequencies. However, experimental studies of composites in this direction do not yet exist to our best knowledge. Another important factor is the application of a magnetic field during solidification. Since the direction of easy magnetization coincides with the direction of maximum magnetostriction, this makes it possible to increase the number of particles with direction  $\langle 100 \rangle$  or close to it along one of the outer directions of the composite (along which the magnetic field was applied). In the example of magnetostrictive composites based on Terfenol-D, the effectiveness of this approach was shown [95]. In the case of Fe-Ga, this also leads to a significant increase in magnetostriction, in some cases more than three times compared to un-oriented samples [87,93]. This effect is highly dependent on the morphology and particle size, as well as the alloy–epoxy ratio and solidification conditions, as well as the magnitude of the applied magnetic field. There are two main driving forces for the orientation of particles in a magnetic field, namely magneto crystalline anisotropy and shape anisotropy [96], therefore, under certain conditions (for example, Fe-Ga in the form of flakes with  $\langle 111 \rangle$  in plane directions), the application of a magnetic field may not be effective in increasing magnetostriction. Another way to improve the functional properties of composites is to select particles of a certain size. However, it should be noted that from the point of view of the effect of particle size on the magnetostriction of composites based on Fe-Ga, the data presented in the literature diverge. According to the data [84] the highest magnetostriction has composites based on Fe-Ga particles with a size below 25  $\mu\text{m}$  in comparison with particles 25–40  $\mu\text{m}$  and 40–75  $\mu\text{m}$ . On the other hand, Walters et al. [86] reported that the highest magnetostriction has composite based on 50–100  $\mu\text{m}$  particles in comparison with the 20–50 and 100–200  $\mu\text{m}$  ones. Finally, the authors of [95] compared composites based on particles with sizes 50 and 75  $\mu\text{m}$  and showed that the latter ones have significantly higher magnetostriction. In general, the mechanism of the effect of particle size on the magnetostriction of Fe-Ga/epoxy composites remains unclear, and further research is required in this direction. Table 2 lists some of the manufacturing parameters of the composites reported in the literature and their saturation magnetostriction values.

**Table 2.** List of some manufacturing parameters such as alloy chemical composition, method of powder preparation, particle size ( $D$ ), epoxy resin content, oriented magnetic field, method of composite fabrication, and saturation magnetostriction value ( $\lambda_s$ ) measured along one of the sample directions.

Alloy	Method of Powder Preparation	$D$ , $\mu\text{m}$	Epoxy Content	Applied Field, T	Method of Composite Fabrication	$\lambda_s$ , ppm	Ref.
Fe <sub>85</sub> Ga <sub>15</sub>	Spark erosion	20–25	52% vol.	0.2	Curing in mold at 100 °C	34	[91]
Fe <sub>85</sub> Ga <sub>15</sub>	Spark erosion	<20	52% vol.	0.2	Curing in mold at 100 °C	15	[91]
Fe <sub>83.7</sub> Ga <sub>16.3</sub>	Spark erosion	20–25	52% vol.	0.2	Curing in mold at 100 °C	35	[91]

Table 2. Cont.

Alloy	Method of Powder Preparation	D, $\mu\text{m}$	Epoxy Content	Applied Field, T	Method of Composite Fabrication	$\lambda_s$ , ppm	Ref.
$\text{Fe}_{81.1}\text{Ga}_{18.9}$	Spark erosion	20–25	52% vol.	0.2	Curing in mold at 100 °C	54	[91]
$\text{Fe}_{81.4}\text{Ga}_{18.6}$	Gas atomization	<25	30.9% vol.	2	Compaction at 271 MPa + curing at 170 °C	58	[84]
$\text{Fe}_{81.4}\text{Ga}_{18.6}$	Gas atomization	25–40	32.6% vol.	2	Compaction at 271 MPa + curing at 170 °C	49	[84]
$\text{Fe}_{81.4}\text{Ga}_{18.6}$	Gas atomization	40–75	34.4% vol.	2	Compaction at 271 MPa + curing at 170 °C	45	[84]
$\text{Fe}_{80}\text{Ga}_{20}$	Blade milling	20–50	20% vol.	-	Compaction at 120 MPa (24 h) + curing at 80 °C	96	[86]
$\text{Fe}_{80}\text{Ga}_{20}$	Blade milling	50–100	20% vol.	-	Compaction at 120 MPa (24 h) + curing at 80 °C	225	[86]
$\text{Fe}_{80}\text{Ga}_{20}$	Blade milling	100–200	20% vol.	-	Compaction at 120 MPa (24 h) + curing at 80 °C	160	[86]
$\text{Fe}_{80}\text{Ga}_{20}$	Ball milling	225 (flakes)	40 wt.%	-	Compaction at 500 MPa	53	[87]
$\text{Fe}_{80}\text{Ga}_{20}$	Ball milling	225 (flakes)	40 wt.%	0.2	Compaction at 500 MPa	70	[87]
$\text{Fe}_{83}\text{Ga}_{17}$	Ball milling	<75	25 wt.%	-	Compaction between two pieces of plexiglass + air drying	34	[94]
$\text{Fe}_{83}\text{Ga}_{17}$	Ball milling	<75	25 wt.%	1	Compaction between two pieces of plexiglass + air drying	60	[94]
$(\text{Fe}_{83}\text{Ga}_{17})_{97}\text{Y}_3$	Ball milling	<75	25 wt.%	-	The same	32	[94]
$(\text{Fe}_{83}\text{Ga}_{17})_{97}\text{Y}_3$	Ball milling	<75	25 wt.%	1	The same	112	[94]
$\text{Fe}_{83}\text{Ga}_{17}$	Ball milling	<75	33 wt.%	-	The same	42	[93]
$\text{Fe}_{83}\text{Ga}_{17}$	Ball milling	<75	33 wt.%	1	The same	73	[93]
$\text{Fe}_{83}\text{Ga}_{17}$	Ball milling	<75	50 wt.%	1	The same	49	[93]
$(\text{Fe}_{83}\text{Ga}_{17})_{99.8}\text{Pr}_{0.2}$	Ball milling	<75	33 wt.%	-	The same	36	[93]
$(\text{Fe}_{83}\text{Ga}_{17})_{99.8}\text{Pr}_{0.2}$	Ball milling	<75	33 wt.%	1	The same	168	[93]
$(\text{Fe}_{83}\text{Ga}_{17})_{99.8}\text{Pr}_{0.2}$	Ball milling	<75	50 wt.%	1	The same	137	[93]
$(\text{Fe}_{83}\text{Ga}_{17})_{99}\text{Pr}_1$	Ball milling	<75	33 wt.%	-	The same	75	[93]
$(\text{Fe}_{83}\text{Ga}_{17})_{99}\text{Pr}_1$	Ball milling	<75	33 wt.%	1	The same	320	[93]
$(\text{Fe}_{83}\text{Ga}_{17})_{99}\text{Pr}_1$	Ball milling	<75	50 wt.%	1	The same	251	[93]

It is seen that the reported data are very heterogeneous. The composition of the alloy, the methods of manufacturing the powder, the particle size, and the content of epoxy resin

are different, which is also indicated in various ways (vol. or wt.%), which is not possible to recalculate without information on the density of the components used. Composite fabrication parameters also vary greatly. All this is superimposed on different equipment and protocols used by different research groups in measuring magnetostriction, which also causes significant discrepancies. For example, round-robin tests of magnetostriction of the same FeSi samples by the same method in nine independent laboratories showed deviation in values up to 5% [97]. Obviously, in the case of more complex objects such as Fe-Ga/epoxy composites and the use of different methods, this discrepancy can be exacerbated. All this makes it impossible to analyze the correlations between manufacturing parameters and magnetostriction in composites using data that exists today.

In addition, it should be noted that some of the data presented look doubtful. In particular, a reported magnetostriction value of about 225 ppm for the composite Fe<sub>80</sub>Ga<sub>20</sub>/20% vol. epoxy [86]. There are no obvious physical reasons for a metal/epoxy composite with a relatively high epoxy content to exhibit magnetostriction close to a single crystal. In addition, in none of the other experiments, such high values were obtained on a binary alloy, regardless of the manufacturing parameters.

#### 4. Prospects and Directions for Further Research

In this section, we discuss the steps that need to be taken to move closer to the widespread practical use of the Fe-Ga alloy for elevated frequency applications. But before that, let us consider the advantages and disadvantages of the two described approaches that can be used to create energy-efficient magnetostrictive devices. In the case of laminated stacks, the advantages are high magnetostriction in the sheets, which, in the presence of the required texture, is close to the value for a single crystal. In addition, such objects, subject to the optimal structure in the sheets from which they are made, are suitable for use in a wide range of temperatures and under mechanical stress. Disadvantages are the technological difficulties that arise during the rolling of this alloy, as well as the difficulty of creating an optimal structure and crystallographic texture. As for Fe-Ga/epoxy composites, their manufacture is a much cheaper process; in addition, it is possible to directly obtain products of the required shape, avoiding additional metalworking operations and, as a result, unnecessary consumption of material. In addition, due to their structure, such objects will obviously have better frequency stability and lower eddy current losses compared to laminated stacks. The disadvantages are the inability to work at elevated temperatures, as a rule, lower values of magnetostriction than in sheets, and higher saturation fields due to the demagnetizing factor of individual ferromagnetic particles in the composite structure. Thus, the choice of an appropriate method for creating bulk magnetostrictive products for operation at elevated frequencies should be based on the expected operating conditions.

In the context of magnetostrictive applications at elevated frequency, not only magnetic properties are important, but also mechanical properties, such as fatigue behavior. To our knowledge, the fatigue performance of Fe-Ga was studied on ingots only [98,99]. There are no such studies for sheets; however, we can assume that Fe-Ga sheets (especially obtained by primary recrystallization technology) have a much better fatigue performance as well as other mechanical properties compared to Fe-Ga/epoxy composites.

In both of these directions, unsolved problems remain, which should form the basis of further research. As shown in this review, at the moment, the main attention is focused on the issue of creating thin Fe-Ga sheets with a given structure and optimal properties. The next step is the creation of laminated stacks on their basis and a detailed analysis of their properties at working frequencies (magnetostriction, permeability, and core losses). To our best knowledge, there are no such studies yet. In addition, a promising direction is the rolling of alloys of the FeGaRE system, which are superior to the binary Fe-Ga alloy in terms of properties. However, such studies began to appear only this year [100] and a little earlier for similar alloys FeAlRE [101], which does not yet make it possible to draw unambiguous conclusions about how suitable such alloys are for rolling and the possibility of creating the necessary crystallographic texture in them.

As for Fe-Ga/insulator composites, this direction remains less studied compared to Fe-Ga sheets. Approaches and parameters used in published works differ greatly, which makes it impossible to establish correlations in the chain: manufacturing parameters–structure–properties. This, in turn, does not make it possible to develop optimal modes for the manufacture of composites with desired properties. To solve this problem, further complex experimental studies are needed, aimed primarily at establishing the influence of individual parameters on functional properties. Another problem is that in the Fe-Ga-based magnetostrictive composites being developed, only magnetostriction is controlled, while other functionally significant properties, such as core losses or frequency stability of permeability, are ignored. This does not allow us to evaluate the prospects for using such objects at different frequencies.

Thus, for the further development of this direction, it is required to focus on the identified problems, which will make it possible to significantly move towards the widespread practical use of the Fe-Ga alloy in magnetostrictive devices operating at elevated frequencies.

## 5. Conclusions

This review considers the features and prospects of using the Fe-Ga alloy for magnetostrictive applications at elevated frequencies. In this context, Fe-Ga has been shown to have the most attractive combination of properties compared to other popular magnetostrictive alloys such as FeCo and TbDyFe. It combines higher electrical resistivity and magnetic permeability, as well as lower coercivity and saturation field. Two technologies for reducing eddy current losses in the case of Fe-Ga are considered, such as the creation of textured sheets by rolling and recrystallization, as well as the creation of metal/epoxy composites. The creation of a favorable texture in Fe-Ga sheets providing high magnetostriction is possible due to both secondary recrystallization and primary recrystallization under certain conditions, which opens up great opportunities for optimizing their structure. Composites based on Fe-Ga can also be a promising direction with their own advantages; however, for this, it is necessary to develop optimal parameters for their manufacture, which has not yet been done.

**Author Contributions:** Conceptualization, V.M. and R.B.; investigation, V.M.; resources, R.B. and M.F.; data curation, V.M.; writing—original draft preparation, V.M.; writing—review and editing, R.B.; project administration, M.F.; funding acquisition, M.F. All authors have read and agreed to the published version of the manuscript.

**Funding:** The research was supported by the Mobility and Reintegration Programme of the Slovak Academy of Sciences (MoRePro) number 19MRP0061, Slovak Research and Development Agency under the contract APVV-20-0072, and by the Scientific Grant Agency of the Ministry of Education of the Slovak Republic and the Slovak Academy of Sciences—project VEGA 2/0029/21. This work was supported by the Grant of the President of the Russian Federation for young scientists (number MK-344.2022.4) and within the framework of the state task of the Ministry of Science and Higher Education of the Russian Federation (“Magnet” 122021000034-9).

**Data Availability Statement:** No new data were created in this study. Data sharing is not applicable to this article.

**Conflicts of Interest:** The authors declare no conflict of interest.

## References

1. Hristoforou, E.; Ktena, A.; Gong, S. Magnetic Sensors: Taxonomy, Applications, and New Trends. *IEEE Trans. Magn.* **2019**, *55*, 1–14. [CrossRef]
2. Claeysen, F.; Lhermet, N.; Le Letty, R.L.; Bouchilloux, P. Actuators, transducers and motors based on giant magnetostrictive materials. *J. Alloys Compd.* **1997**, *258*, 61–73. [CrossRef]
3. Dapino, M.J.; Deng, Z.; Calkins, F.T.; Flatau, A.B. Magnetostrictive Devices. In *Wiley Encyclopedia of Electrical and Electronics Engineering*; Webster, J.G., Ed.; 2016. Available online: <https://onlinelibrary.wiley.com/doi/10.1002/047134608X.W4549.pub2> (accessed on 4 September 2023).
4. Akinaga, H. Recent advances and future prospects in energy harvesting technologies. *Jpn. J. Appl. Phys.* **2020**, *59*, 110201. [CrossRef]

5. Gao, C.; Zeng, Z.; Peng, S.; Shuai, C. Magnetostrictive alloys: Promising materials for biomedical applications. *Bioact. Mater.* **2022**, *8*, 177–195. [[CrossRef](#)] [[PubMed](#)]
6. Pradhan, G.; Celegato, F.; Barrera, G.; Olivetti, E.S.; Coisson, M.; Hajduček, J.; Arregi, J.A.; Čelko, L.; Uhlř, V.; Rizzi, P.; et al. Magnetic properties of FeGa/Kapton for flexible electronics. *Sci. Rep.* **2022**, *12*, 17503. [[CrossRef](#)] [[PubMed](#)]
7. Yermakov, A.; Thompson, A.; Coaty, C.; Sabo, R.; Law, C.T.; Elhajjar, R. Flexible Magnetostrictive Nanocellulose Membranes for Actuation, Sensing, and Energy Harvesting Applications. *Front. Mater.* **2020**, *7*, 38. [[CrossRef](#)]
8. Golovin, I.S.; Palacheva, V.V.; Mohamed, A.K.; Balagurov, A.M. Structure and Properties of Fe–Ga Alloys as Promising Materials for Electronics. *Phys. Met. Metallogr.* **2020**, *121*, 851–893. [[CrossRef](#)]
9. Ma, T.; Gou, J.; Hu, S.; Liu, X.; Wu, C.; Ren, S.; Zhao, H.; Xiao, A.; Jiang, C.; Ren, X.; et al. Highly thermal-stable ferromagnetism by a natural composite. *Nat. Commun.* **2017**, *8*, 13937. [[CrossRef](#)]
10. Wang, H.; Zheng, Y.; Liu, J.; Jiang, C.; Li, Y. In vitro corrosion properties and cytocompatibility of Fe-Ga alloys as potential biodegradable metallic materials. *Mater. Sci. Eng. C* **2017**, *71*, 60–66. [[CrossRef](#)]
11. Clark, A.E.; Restorff, J.B.; Wun-Fogle, M.; Lograsso, T.A.; Schlagel, D.L. Magnetostrictive Properties of Body-Centered Cubic. *IEEE Trans. Magn.* **2000**, *36*, 3238–3240. [[CrossRef](#)]
12. Ueno, T.; Summers, E.; Wun-Fogle, M.; Higuchi, T. Micro-magnetostrictive vibrator using iron-gallium alloy. *Sens. Actuators A Phys.* **2008**, *148*, 280–284. [[CrossRef](#)]
13. Yao, Y.; Pan, Y.; Liu, S. Power ultrasound and its applications: A state-of-the-art review. *Ultrason. Sonochem.* **2020**, *62*, 104722. [[CrossRef](#)] [[PubMed](#)]
14. Pan, Y.; Mo, X.; Li, Y.; Chai, Y.; Liu, Y.; Zhang, Y. A magnetostrictive underwater transducer directly driven by Iron-Gallium alloy (Galfenol) without bias magnetic field. In Proceedings of the OCEANS 2015-MTS/IEEE Washington, Washington, DC, USA, 19–22 October 2015; pp. 5–8. [[CrossRef](#)]
15. Ueno, T.; Miura, H.; Yamada, S. Evaluation of a miniature magnetostrictive actuator using Galfenol under tensile stress. *J. Phys. D Appl. Phys.* **2011**, *44*, 2–7. [[CrossRef](#)]
16. Clemente, C.S.; Davino, D. Modeling and characterization of a kinetic energy harvesting device based on galfenol. *Materials* **2019**, *12*, 3199. [[CrossRef](#)] [[PubMed](#)]
17. Deng, Z.; Dapino, M.J. Modeling and design of Galfenol unimorph energy harvesters. *Smart Mater. Struct.* **2015**, *24*, 125019. [[CrossRef](#)]
18. Ahmed, U.; Aydin, U.; Zucca, M.; Palumbo, S.; Kouhia, R.; Rasilo, P. Modeling a Fe-Ga energy harvester fitted with magnetic closure using 3D magneto-mechanical finite element model. *J. Magn. Magn. Mater.* **2020**, *500*, 166390. [[CrossRef](#)]
19. Palumbo, S.; Rasilo, P.; Zucca, M. Experimental investigation on a Fe-Ga close yoke vibrational harvester by matching magnetic and mechanical biases. *J. Magn. Magn. Mater.* **2019**, *469*, 354–363. [[CrossRef](#)]
20. Xing, Q.; Lograsso, T.A. Effect of cooling rate on magnetoelasticity and short-range order in Fe-Ga alloys. *Scr. Mater.* **2011**, *65*, 359–362. [[CrossRef](#)]
21. He, Y.; Jiang, C.; Wu, W.; Wang, B.; Duan, H.; Wang, H.; Zhang, T.; Wang, J.; Liu, J.; Zhang, Z.; et al. Giant heterogeneous magnetostriction in Fe-Ga alloys: Effect of trace element doping. *Acta Mater.* **2016**, *109*, 177–186. [[CrossRef](#)]
22. Meng, C.; Wu, Y.; Jiang, C. Design of high ductility FeGa magnetostrictive alloys: Tb doping and directional solidification. *Mater. Des.* **2017**, *130*, 183–189. [[CrossRef](#)]
23. Chen, Y.; Fu, Z.; Wu, Y.; Xu, Y.; Xiao, Y.; Wang, J.; Zhang, R.; Jiang, C. Giant heterogeneous magnetostriction induced by charge accumulation-mediated nanoinclusion formation in dual-phase nanostructured systems. *Acta Mater.* **2021**, *213*, 116975. [[CrossRef](#)]
24. Adelani, M.O.; Olive-Méndez, S.F.; Espinosa-Magaña, F.; Matutes-Aquino, J.A.; Grijalva-Castillo, M.C. Structural, magnetic and electronic properties of Fe-Ga-Tb<sub>x</sub> (0 ≤ x ≤ 1.85) alloys: Density-functional theory study. *J. Alloys Compd.* **2021**, *857*, 157540. [[CrossRef](#)]
25. Jin, T.; Wang, H.; Chen, Y.; Li, T.; Wang, J.; Jiang, C. Evolution of nanoheterogeneities and correlative influence on magnetostriction in FeGa-based magnetostrictive alloys. *Mater. Charact.* **2022**, *186*, 111780. [[CrossRef](#)]
26. Zhao, Y.; Li, J.; Liu, Y.; Li, M.; Jiang, H.; Mu, X.; Bao, X.; Gao, X. Magnetostriction and structure characteristics of Co<sub>70</sub>Fe<sub>30</sub> alloy prepared by directional solidification. *J. Magn. Magn. Mater.* **2018**, *451*, 587–593. [[CrossRef](#)]
27. Summers, E.M.; Lograsso, T.A.; Wun-Fogle, M. Magnetostriction of binary and ternary Fe-Ga alloys. *J. Mater. Sci.* **2007**, *42*, 9582–9594. [[CrossRef](#)]
28. Steiner, J.; Lisfi, A.; Kakeshita, T.; Fukuda, T.; Wuttig, M. Unique magnetostriction of Fe<sub>68.8</sub>Pd<sub>31.2</sub> attributable to twinning. *Sci. Rep.* **2016**, *6*, 34259. [[CrossRef](#)]
29. Petculescu, G.; Leblanc, J.B.; Wun-Fogle, M.; Restorff, J.B.; Burton, W.C.; Cao, J.X.; Wu, R.Q.; Yuhasz, W.M.; Lograsso, T.A.; Clark, A.E. Magnetoelasticity of Fe<sub>100-x</sub>Ge<sub>x</sub> (5 < x < 18) single crystals from 81 K to 300 K. *IEEE Trans. Magn.* **2009**, *45*, 4149–4152. [[CrossRef](#)]
30. Chen, Y.; Wang, J.; Yang, B.; Liu, J.; Jiang, C. Morphology evolution and enhanced magnetostriction of (Fe<sub>0.81</sub>Ga<sub>0.19</sub>)<sub>99.9</sub>Tb<sub>0.1</sub> crystals prepared by liquid metal cooling Bridgman directional solidification. *J. Alloys Compd.* **2021**, *856*, 158166. [[CrossRef](#)]
31. Liu, Y.; Li, J.; Gao, X. Effect of Al substitution for Ga on the mechanical properties of directional solidified Fe-Ga alloys. *J. Magn. Magn. Mater.* **2017**, *423*, 245–249. [[CrossRef](#)]
32. Snodgrass, J.D.; McMasters, O.D. Optimized TERFENOL-D manufacturing processes. *J. Alloys Compd.* **1997**, *258*, 24–29. [[CrossRef](#)]

33. Yang, Z.; Li, J.; Zhou, Z.; Gong, J.; Bao, X.; Gao, X. Recent Advances in Magnetostrictive Tb-Dy-Fe Alloys. *Metals* **2022**, *12*, 341. [[CrossRef](#)]
34. Weng, L.; Li, W.; Sun, Y.; Huang, W.; Wang, B. High frequency characterization of Galfenol minor flux density loops. *AIP Adv.* **2017**, *7*, 056023. [[CrossRef](#)]
35. Huang, W.; Xia, Z.; Guo, P.; Weng, L. Analysis and experimental research on high frequency magnetic properties of different magnetostrictive materials under variable temperature conditions. *AIP Adv.* **2022**, *12*, 035231. [[CrossRef](#)]
36. Birčáková, Z.; Milyutin, V.; Kollár, P.; Fáberová, M.; Bureš, R.; Füzér, J. Magnetic characteristics and core loss separation in magnetostrictive FeGa and FeGaRE (RE = Tb, Y) alloys. *Intermetallics* **2022**, *151*, 107744. [[CrossRef](#)]
37. Zhang, R.; Zhou, C.; Chen, K.; Cao, K.; Zhang, Y.; Tian, F.; Murtaza, A.; Yang, S.; Song, X. Near-zero magnetostriction in magnetostrictive FeCo alloys. *Scr. Mater.* **2021**, *203*, 114043. [[CrossRef](#)]
38. Niu, X.; Li, M.; Wang, Q.; Liu, M.; Wang, B.; Huang, W.; Weng, L.; Sun, Y. Non-contact torque sensor based on magnetostrictive Fe<sub>30</sub>Co<sub>70</sub> alloy. *AIP Adv.* **2022**, *12*, 035112. [[CrossRef](#)]
39. Colaiori, F.; Durin, G.; Zapperi, S. Eddy current damping of a moving domain wall: Beyond the quasistatic approximation. *Phys. Rev. B Condens.* **2007**, *76*, 224416. [[CrossRef](#)]
40. Sondheimer, E.H. The mean free path of electrons in metals. *Adv. Phys.* **2001**, *50*, 499–537. [[CrossRef](#)]
41. Xu, S.F.; Zhang, H.P.; Wang, W.Q.; Guo, S.H.; Zhu, W.; Zhang, Y.H.; Wang, X.L.; Zhao, D.L.; Chen, J.L.; Wu, G.H. Magnetostriction and electrical resistivity of Mn doped Fe<sub>81</sub>Ga<sub>19</sub> alloys. *J. Phys. D Appl. Phys.* **2008**, *41*, 135304. [[CrossRef](#)]
42. Miracle, D.B.; Senkov, O.N. A critical review of high entropy alloys and related concepts. *Acta Mater.* **2017**, *122*, 448–511. [[CrossRef](#)]
43. Milyutin, V.; Birčáková, Z.; Fáberová, M.; Bureš, R.; Kollár, P.; Füzér, J. Effect of Rare-Earth Doping on Dynamic Magnetic Properties of FeGa Alloy. *Mater. Sci. Forum* **2023**, *1081*, 149–154. [[CrossRef](#)]
44. Javed, A.; Szumiata, T.; Morley, N.A.; Gibbs, M.R.J. An investigation of the effect of structural order on magnetostriction and magnetic behavior of Fe–Ga alloy thin films. *Acta Mater.* **2010**, *58*, 4003–4011. [[CrossRef](#)]
45. Boesenberg, A.J.; Restorff, J.B.; Wun-Fogle, M.; Sailsbury, H.; Summers, E. Texture development in Galfenol wire. *J. Appl. Phys.* **2013**, *113*, 10–13. [[CrossRef](#)]
46. Milyutin, V.A.; Gervasyeva, I.V.; Volkova, E.G.; Alexandrov, A.V.; Cheverikin, V.V.; Mansouri, Y.; Palacheva, V.V.; Golovin, I.S. Texture formation in FeGa alloy at cold hydrostatic extrusion and primary recrystallization. *J. Alloys Compd.* **2020**, *816*, 153283. [[CrossRef](#)]
47. Leuning, N.; Steentjes, S.; Hameyer, K. Effect of grain size and magnetic texture on iron-loss components in NO electrical steel at different frequencies. *J. Magn. Magn. Mater.* **2019**, *469*, 373–382. [[CrossRef](#)]
48. Meloy, R.; Summers, E. Magnetic property–texture relationships in galfenol rolled sheet stacks. *J. Appl. Phys.* **2011**, *109*, 07A930. [[CrossRef](#)]
49. Suzuki, S.; Kawamata, T.; Simura, R.; Asano, S.; Fujieda, S.; Umetsu, R.Y.; Fujita, M.; Imafuku, M.; Kumagai, T.; Fukuda, T. Anisotropy of magnetostriction of functional BCC iron-based alloys. *Mater. Trans.* **2019**, *60*, 2235–2244. [[CrossRef](#)]
50. Mohamed, A.K.; Palacheva, V.V.; Cheverikin, V.V.; Zanaeva, E.N.; Cheng, W.C.; Kulitckii, V.; Divinski, S.; Wilde, G.; Golovin, I.S. The Fe–Ga phase diagram: Revisited. *J. Alloys Compd.* **2020**, *846*, 156486. [[CrossRef](#)]
51. Atulasimha, J.; Flatau, A.B. A review of magnetostrictive iron-gallium alloys. *Smart Mater. Struct.* **2011**, *20*, 043001. [[CrossRef](#)]
52. Na, S.-M.; Flatau, A.B. Single grain growth and large magnetostriction in secondarily recrystallized Fe–Ga thin sheet with sharp Goss (0 1 1)[1 0 0] orientation. *Scr. Mater.* **2012**, *66*, 307–310. [[CrossRef](#)]
53. Fu, Q.; Sha, Y.H.; Zhang, F.; Esling, C.; Zuo, L. Correlative effect of critical parameters for  $\eta$  recrystallization texture development in rolled Fe<sub>81</sub>Ga<sub>19</sub> sheet: Modeling and experiment. *Acta Mater.* **2019**, *167*, 167–180. [[CrossRef](#)]
54. Sun, A.; Liu, J.; Jiang, C. Recrystallization, texture evolution, and magnetostriction behavior of rolled (Fe<sub>81</sub>Ga<sub>19</sub>)<sub>98</sub>B<sub>2</sub> sheets during low-to-high temperature heat treatments. *J. Mater. Sci.* **2014**, *49*, 4565–4575. [[CrossRef](#)]
55. Milyutin, V.A.; Gervasyeva, I.V.; Shishkin, D.A.; Beaunon, E. Structure and texture in rolled Fe<sub>82</sub>Ga<sub>18</sub> and (Fe<sub>82</sub>Ga<sub>18</sub>)<sub>99</sub>B<sub>1</sub> alloys after annealing under high magnetic field. *Phys. B Condens. Matter* **2022**, *639*, 413994. [[CrossRef](#)]
56. Na, S.M.; Smith, M.; Flatau, A.B. Deformation Mechanism and Recrystallization Relationships in Galfenol Single Crystals: On the Origin of Goss and Cube Orientations. *Metall. Mater. Trans. A* **2018**, *49*, 2499–2512. [[CrossRef](#)]
57. Li, J.; Qi, Q.; Yuan, C.; Bao, X.; Gao, X. Selective abnormal growth behavior of Goss grains in magnetostrictive Fe–Ga alloy sheets. *Mater. Trans.* **2016**, *57*, 2083–2088. [[CrossRef](#)]
58. Qi, Q.; Li, J.; Mu, X.; Ding, Z.; Bao, X.; Gao, X. Microstructure evolution, magnetostrictive and mechanical properties of (Fe<sub>83</sub>Ga<sub>17</sub>)<sub>99.9</sub>(NbC)<sub>0.1</sub> alloy ultra-thin sheets. *J. Mater. Sci.* **2020**, *55*, 2226–2238. [[CrossRef](#)]
59. Mansouri, Y.; Cheverikin, V.V.; Palacheva, V.V.; Koshmin, A.N.; Aleshchenko, A.S.; Astakhov, V.A.; Dementeva, O.Y.; Milyutin, V.A.; Golovin, I.S. Texture and Magnetostriction in Warm Rolled and Recrystallized Fe–Ga Alloy. *Phys. Met. Metallogr.* **2021**, *122*, 389–395. [[CrossRef](#)]
60. Li, J.H.; Gao, X.X.; Zhu, J.; Bao, X.Q.; Xia, T.; Zhang, M.C. Ductility, texture and large magnetostriction of Fe–Ga-based sheets. *Scr. Mater.* **2010**, *63*, 246–249. [[CrossRef](#)]
61. Li, J.H.; Gao, X.X.; Xie, J.X.; Yuan, C.; Zhu, J.; Yu, R.B. Recrystallization behavior and magnetostriction under pre-compressive stress of Fe–Ga–B sheets. *Intermetallics* **2012**, *26*, 66–71. [[CrossRef](#)]

62. Milyutin, V.A.; Gervasyeva, I.V. Formation of crystallographic texture in Fe-Ga alloys during various types of plastic deformation and primary recrystallization. *Mater. Today Commun.* **2021**, *27*, 102193. [[CrossRef](#)]
63. He, Z.; Sha, Y.; Zhang, F.; Lin, F.; Zuo, L. Development of strong  $\eta$  fiber recrystallization texture in rolled Fe<sub>81</sub>Ga<sub>19</sub> thin sheet. *Metall. Mater. Trans. A* **2014**, *45*, 129–133. [[CrossRef](#)]
64. Yuan, C.; Li, J.; Bao, X.; Gao, X. Influence of annealing process on texture evolution and magnetostriction in rolled Fe-Ga based alloys. *J. Magn. Magn. Mater.* **2014**, *362*, 154–158. [[CrossRef](#)]
65. Gervasyeva, I.V.; Milyutin, V.A. Texture formation under rolling and primary recrystallization in Fe<sub>86</sub>Ga<sub>14</sub> alloy. *Lett. Mater.* **2018**, *8*, 341–345. [[CrossRef](#)]
66. Li, J.; Gao, X.; Zhu, J.; He, C.; Qiao, J.; Zhang, M. Texture evolution and magnetostriction in rolled (Fe<sub>81</sub>Ga<sub>19</sub>)<sub>99</sub>Nb<sub>1</sub> alloy. *J. Alloys Compd.* **2009**, *476*, 529–533. [[CrossRef](#)]
67. Yuan, C.; Li, J.; Zhang, W.; Bao, X.; Gao, X. Secondary recrystallization behavior in the rolled columnar-grained Fe-Ga alloys. *J. Magn. Magn. Mater.* **2015**, *391*, 145–150. [[CrossRef](#)]
68. He, Z.; Sha, Y.; Fu, Q.; Lei, F.; Jin, B.; Zhang, F.; Zuo, L. Sharp Goss texture and magnetostriction in binary Fe<sub>81</sub>Ga<sub>19</sub> sheets. *J. Magn. Magn. Mater.* **2016**, *417*, 321–326. [[CrossRef](#)]
69. Li, J.; Yuan, C.; Qi, Q.; Bao, X.; Gao, X. Effect of initial oriented columnar grains on the texture evolution and magnetostriction in Fe-Ga rolled sheets. *Metals* **2017**, *7*, 36. [[CrossRef](#)]
70. Fu, Q.; Sha, Y.; He, Z.; Lei, F.; Zhang, F.; Zuo, L. Recrystallization texture and magnetostriction in binary Fe<sub>81</sub>Ga<sub>19</sub> sheets. *Jinshu Xuebao/Acta Metall. Sin.* **2017**, *53*, 90–96. [[CrossRef](#)]
71. Li, J.; Liu, Y.; Li, X.; Mu, X.; Bao, X.; Gao, X. Effects of rolling conditions on recrystallization microstructure and texture in magnetostrictive Fe-Ga-Al rolled sheets. *J. Magn. Magn. Mater.* **2018**, *457*, 30–37. [[CrossRef](#)]
72. Xia, Y.; Zhang, Y.; Wu, T.; Wang, N.; Ran, R.; Wang, Y.; Fang, F.; Wang, G. Deformation twinning caused by warm rolling and secondary recrystallization in twin-roll strip casting Fe<sub>81</sub>Ga<sub>19</sub> alloy. *J. Alloys Compd.* **2022**, *922*, 166039. [[CrossRef](#)]
73. Yuan, C.; Gao, X.-X.; Li, J.-H.; Bao, X.-Q. Secondary recrystallization of Goss texture in magnetostrictive Fe-Ga-based sheets. *Rare Met.* **2020**, *39*, 1288–1294. [[CrossRef](#)]
74. He, Z.; Hao, H.; Sha, Y.; Li, W.; Zhang, F.; Zuo, L. Sharp secondary recrystallization and large magnetostriction in Fe<sub>81</sub>Ga<sub>19</sub> sheet induced by composite nanometer-sized inhibitors. *J. Magn. Magn. Mater.* **2019**, *478*, 109–115. [[CrossRef](#)]
75. Van Order, M.; Sinha, S.; Wang, H.; Wu, R.; Gaskell, K.; Flatau, A. Non-Destructive Surface Energy Measurements on (1 0 0) Galfenol. *Adv. Theory Simul.* **2018**, *2*, 1800043. [[CrossRef](#)]
76. Hayakawa, Y. Mechanism of secondary recrystallization of Goss grains in grain-oriented electrical steel. *Sci. Technol. Adv. Mater.* **2017**, *18*, 480–497. [[CrossRef](#)] [[PubMed](#)]
77. Yoo, B.; Pines, D.J. Investigation of the use of uniaxial comb-shaped Galfenol patches for a guided wave-based magnetostrictive phased array sensor. *AIP Adv.* **2018**, *8*, 056641. [[CrossRef](#)]
78. Li, J.H.; Gao, X.X.; Zhu, J.; Bao, X.Q.; Zhang, M.C.; Zhao, N. Effects of magnetic field annealing on recrystallization texture and magnetostriction in as-rolled Fe-Ga based alloy. In Proceedings of the Materials Science and Technology Conference and Exhibition (MS and T'09), Pittsburgh, PA, USA, 25–29 October 2009; pp. 115–123.
79. Khachatryan, A.G.; Viehland, D. Structurally heterogeneous model of extrinsic magnetostriction for Fe-Ga and similar magnetic alloys: Part II. Giant magnetostriction and elastic softening. *Metall. Mater. Trans. A* **2007**, *38*, 2317–2328. [[CrossRef](#)]
80. Gou, J.; Ma, T.; Liu, X.; Zhang, C.; Sun, L.; Sun, G.; Xia, W.; Ren, X. Large and sensitive magnetostriction in ferromagnetic composites with nanodispersive precipitates. *NPG Asia Mater.* **2021**, *13*, 1–13. [[CrossRef](#)]
81. Elhajjar, R.; Law, C.T.; Pegoretti, A. Magnetostrictive polymer composites: Recent advances in materials, structures and properties. *Prog. Mater. Sci.* **2018**, *97*, 204–229. [[CrossRef](#)]
82. Bira, N.; Dhagat, P.; Davidson, J.R. A Review of Magnetic Elastomers and Their Role in Soft Robotics. *Front. Robot. AI* **2020**, *7*, 588391. [[CrossRef](#)]
83. Yoo, B.; Na, S.M.; Flatau, A.B.; Pines, D.J. Ultrasonic guided wave sensing performance of a magnetostrictive transducer using Galfenol flakes-polymer composite patches. *J. Appl. Phys.* **2015**, *117*, 17A916. [[CrossRef](#)]
84. Li, J.; Gao, X.; Zhu, J.; Jia, J.; Zhang, M. The microstructure of Fe-Ga powders and magnetostriction of bonded composites. *Scr. Mater.* **2009**, *61*, 557–560. [[CrossRef](#)]
85. Yoo, B.; Na, S.M.; Flatau, A.B.; Pines, D.J. Directional magnetostrictive patch transducer based on Galfenol's anisotropic magnetostriction feature. *Smart Mater. Struct.* **2014**, *23*, 95035. [[CrossRef](#)]
86. Walters, K.; Busbridge, S.; Walters, S. Magnetic properties of epoxy-bonded iron-gallium particulate composites. *Smart Mater. Struct.* **2013**, *22*, 025009. [[CrossRef](#)]
87. Na, S.-M.; Park, J.-J.; Lee, S.; Jeong, S.-Y.; Flatau, A.B. Magnetic and structural anisotropic properties of magnetostrictive Fe-Ga flake particles and their epoxy-bonded composites. *Mater. Lett.* **2018**, *213*, 326–330. [[CrossRef](#)]
88. Kiseleva, T.; Zholudev, S.; Novakova, A.; Grigoryeva, T. The enhanced magnetodeformational effect in Galfenol/polyurethane nanocomposites by the arrangement of particle chains. *Compos. Struct.* **2016**, *138*, 12–16. [[CrossRef](#)]
89. Riesgo, G.; Elbaile, L.; Carrizo, J.; García, G.; Crespo, R.D.; García, M.A.; Torres, Y.; García, J.A. Villari effect in silicone/FeGa composites. *Bull. Mater. Sci.* **2019**, *42*, 1–7. [[CrossRef](#)]
90. Milyutin, V.A.; Bures, R.; Faberova, M.; Kromka, F. Effect of Milling Parameters on Size, Morphology, and Structure of Fe-Ga Binary Alloy Powder. *J. Mater. Eng. Perform.* **2023**, *32*, 3839–3848. [[CrossRef](#)]

91. Hong, J.I.; Solomon, V.C.; Smith, D.J.; Parker, F.T.; Summers, E.M.; Berkowitz, A.E. One-step production of optimized Fe-Ga particles by spark erosion. *Appl. Phys. Lett.* **2006**, *89*, 16–19. [[CrossRef](#)]
92. Taheri, P.; Barua, R.; Hsu, J.; Zamanpour, M.; Chen, Y.; Harris, V.G. Structure, magnetism, and magnetostrictive properties of mechanically alloyed Fe<sub>81</sub>Ga<sub>19</sub>. *J. Alloys Compd.* **2016**, *661*, 306–311. [[CrossRef](#)]
93. Zhao, X.; Tian, X.; Yao, Z.; Zhao, L.; Wang, R.; Yan, J.; Liu, X. Flexible Pr-Doped Fe–Ga Composite Materials: Preparation, Microstructure, and Magnetostrictive Properties. *Adv. Eng. Mater.* **2020**, *22*, 2000080. [[CrossRef](#)]
94. Zhao, X.; Zhao, L.; Wang, R.; Yan, J.; Tian, X.; Yao, Z.; Tegus, O. The microstructure, preferred orientation and magnetostriction of Y doped Fe-Ga magnetostrictive composite materials. *J. Magn. Magn. Mater.* **2019**, *491*, 165568. [[CrossRef](#)]
95. Dong, X.; Ou, J.; Guan, X.; Qi, M. Optimal orientation field to manufacture magnetostrictive composites with high magnetostrictive performance. *J. Magn. Magn. Mater.* **2010**, *322*, 3648–3652. [[CrossRef](#)]
96. Milyutin, V.A.; Gervasyeva, I.V. Thermally activated transformations in alloys with different type of magnetic ordering under high magnetic field. *J. Magn. Magn. Mater.* **2019**, *492*, 165654. [[CrossRef](#)]
97. Kobori, J.; Takahashi, Y.; Fujiwara, K. The international round robin test of magnetostriction measurement of grain-oriented electrical steel by means of a single sheet tester and an optical sensor. *J. Magn. Magn. Mater.* **2020**, *513*, 166541. [[CrossRef](#)]
98. Holsworth, D.I.; Duquesnay, D.L. Fatigue properties of Galfenol steels. *Int. J. Fatigue* **2019**, *128*, 105177. [[CrossRef](#)]
99. Holsworth, D.I.; Duquesnay, D.L. The effects of hot iso-static pressing on the porosity and fatigue properties of Galfenol steels. *Int. J. Fatigue* **2020**, *131*, 105325. [[CrossRef](#)]
100. He, Z.; Mi, C.; Sha, Y.; Chen, S.; Zhu, X.; Chen, L.; Zuo, L. Enhanced magnetostriction of rolled (Fe<sub>81</sub>Ga<sub>19</sub>)<sub>99.93</sub>Tb<sub>0.07</sub> thin sheet by synergy strategy of secondary recrystallization and trace Tb-doping. *J. Alloys Compd.* **2023**, *942*, 169108. [[CrossRef](#)]
101. Palacheva, V.V.; Mochugovskiy, A.G.; Chubov, D.G.; Koshmin, A.N.; Cheverikin, V.V.; Cifre, J. Influence of mechanical and heat treatment on structure evolution and functional properties of Fe-Al-Tb alloys. *Mater. Lett.* **2022**, *310*, 131521. [[CrossRef](#)]

**Disclaimer/Publisher's Note:** The statements, opinions and data contained in all publications are solely those of the individual author(s) and contributor(s) and not of MDPI and/or the editor(s). MDPI and/or the editor(s) disclaim responsibility for any injury to people or property resulting from any ideas, methods, instructions or products referred to in the content.